



iJRASET

International Journal For Research in
Applied Science and Engineering Technology



INTERNATIONAL JOURNAL FOR RESEARCH

IN APPLIED SCIENCE & ENGINEERING TECHNOLOGY

Volume: 6

Issue: II

Month of publication: February 2018

DOI:

www.ijraset.com

Call:  08813907089

E-mail ID: ijraset@gmail.com

A Report on CTAB Stabilized CuS Nanostructures with Enhanced Structural, Morphological and Electrochemical Properties

Surekha Podili¹, D. Geetha², P.S. Ramesh³

^{1,2} Department of Physics, ³ Department of Physics (DDE Wings), Annamalai University, Chidambaram, Annamalai Nagar 608002, Tamilnadu, India.

Abstract: In this study, we proposed porous copper sulfide (CuS) nano flower by hydrothermal route. Cationic surfactant cetyl trimethyl ammonium bromide (CTAB) was used as stabilizer and copper nitrate as precursors, thiourea as sulfur source and ethylene glycol as solvent. CuS nano crystals were prepared by adding 3 different CTAB concentration viz., 0.05, 0.07 and 0.1 mM at constant temperature 130°C. Structural, morphological and chemical composition of the as-synthesized samples was thoroughly characterized by XRD, SEM/EDS, TEM and XPS techniques respectively. The SEM and TEM images demonstrate flower like nanostructures and also these samples were utilized for electrochemical study by coated the sample on glassy carbon electrode (GCE). The electrochemical performance of the as-synthesized CTAB/CuS material was studied by cyclic voltammetry (CV). These results demonstrate that CTAB (0.1mM)/CuS electrode delivered a high specific capacitance of 328.26 Fg⁻¹ in a 2M KOH aqueous electrolyte at 5mV/s and indicating their potential application as promising electrode materials for super capacitors.

Keywords: Porous CuS; nanoflower; Electrode material; specific capacitance

I. INTRODUCTION

Capacitive energy storage systems have significant interest and importance due to higher power density (10-20 times), a fast charge discharge mechanism and extensive life cycles compared with batteries. The device connecting capacitive energy storage mechanism is called electrochemical capacitor e.g. EDLC, Supercapacitor etc. These power sources were used in electric vehicles, memory backups or back-up supplies to protect against power failure. The EDLC store the charge electro statically and the active materials are stable [1-4].

Normally carbon materials are used because which has high specific surface area (1000 – 2000 m²g⁻¹), good conductivity flexible and availability in different forms. However the effect of electrostatic surface charging mechanism, carbon materials suffer from limited energy density. In contract, the supercapacitors show higher energy density than the EDLC. In supercapacitors, the charges arise due to fact, reversible redox processes going on electrode surface. Some oxide materials possess exhibits higher C_s than that of conventional carbon materials. This has begun to investigate for low-priced alternate electrode materials having excellent capacitance and longer life time [5-7].

In recent times, metal sulfides have been confirmed to the materials of choice for high performance supercapacitors. Metal sulfides have been intensively researched in applications for fuel cells, solar cells and Li-ion batteries in view of their excellent performance [8-10]. Nowadays metal sulfides have prospective application to supercapacitors due to chemical stability, large surface area and conductivity [11, 12]. The metal sulfide nanostructures such as Zinc Sulfide, Cupper Sulfide and Cobalt Sulfide were used as electrode materials for energy storage applications [13-15]. The subsistence of two or more valance states of metal constituents present in sulfides and the sulfur having high theoretical capacity than that of oxides and it can provide better capacitance behavior. The covellite copper sulfide is exhaustive studied material attributable to great potential applications in several fields such as photocatalysis, low-temperature superconductors, super ionic materials, chemical sensors and thermoelectric cooling materials [16-20]. Also CuS as electrode material for supercapacitor owing to its high capacitive behavior, large surface area and low cost also may enhance its performance by improving the preparative methods. For practical application of high power density devices, the powder forms yield better volumetric energy density than films. The transition metal sulfides were good accessibility for redox reactions in supercapacitors [21]. Compared with other metal oxides, the copper mono sulfide is easier, inexpensive and it has higher hole mobility.

From the literature studies, the specific capacitance of CuS strongly depends on the morphology, surface area and preparation methods. Because supercapacitance is an interfacial phenomenon, best way to improve the charge storage capacity is to increase the specific surface area of the materials with optimum pore distribution. Surfactant stabilized synthesis method of CuS may achieve this property. The mesoporous systems with large surface areas are expected the ion transport within the pore system, thus increasing the electroactive material- electrolyte interface area, which may enhances electrochemical performance.

Here, in this report, CuS electrodes were prepared via effortless and low cost hydrothermal route using different concentrations of cationic surfactant (CTAB) as structure promising agent. The important novelty is that there is no any researchers use flower like mesoporous nanostructures as the electrode material to attain high C_s compared to spherical CuS nanostructures. The electrochemical behavior of the CTAB stabilized CuS were investigated as electrode material for supercapacitors in 2M KOH electrolyte solution. Therefore, these can be proposed as good energy storage devices due to the high exchange of ions at the interface. CTAB (0.1mM)-CuS nanostructures have been explored using cyclic voltammetry (CV). These techniques provide the higher C_s which was considerably superior to the earlier reports. The novel CTAB (0.1mM)-CuS electrode reveals high specific capacitance.

II. EXPERIMENTAL SECTIONS

A. Reagents.

Copper nitrate trihydrate ($\text{Cu}(\text{NO}_3)_2 \cdot 3\text{H}_2\text{O}$), Thiourea ($\text{Tu, Sc}(\text{NH}_2)_2$), Ethylene Glycol (EG) and Cetyl trimethyl ammonium bromide (CTAB) from SD fine. All chemicals were of analytical grade and were used without further purification.

B. Synthesis of CuS Nanostructures.

In a typical procedure, 1mM of $\text{Cu}(\text{NO}_3)_2 \cdot 3\text{H}_2\text{O}$, 2 mM of $\text{Tu, Sc}(\text{NH}_2)_2$ and different concentrations of CTAB were dissolved in 40 ml of EG and magnetic stirring for 50 minutes. The solution into a Teflon-lined autoclave sealed and maintained at 130°C for 10 hrs. The resulting black powder of CTAB-CuS sample washed many times with acetone and de-ionized water then dried at 70°C for 6 hrs.

C. Materials Characterization.

The diffraction patterns were recorded on X'Pert-PRO using $\text{Cu K}\alpha$ radiation. X-ray diffractometer at a scan rate of 1°min^{-1} over the range $20^\circ - 70^\circ$ (2θ) at room temperature. The change in morphology on increasing CTAB concentrations stabilized CuS was inspected through a (JEOL-JSM – 5610 LV with INCA EDS) scanning electron microscope (SEM) and the elemental analysis was studied using EDS. The morphologies were analyzed on a TEM CM-200 transmission electron microscope (TEM). Chemical bonding states were investigated by X-ray photoelectron spectroscopy (Kratos Analytical).

D. Electrochemical Measurements.

The electrode preparation and electrochemical characterization techniques used for prepared samples have been discussed in our previous paper [22].

III. RESULTS AND DISCUSSION

In this process, CTAB was selected as a shape inducing agent. Only in the presence of CTAB, CuS well arranged nanostructures were obtained. The concentration of CTAB was tested, the results showed that copper sulfide nanostructures were obtained only in the range of 0.05 to 0.1mM, but when the concentration of CTAB was less than 0.05 or over 0.1mM, the products were agglomerated. The surfactant concentration was varied *viz.*, 0.05, 0.07 and 0.1mM on 1:2 (Cu: S).

It is well known that strong intermolecular forces, such as Vander Waals attraction, $\pi - \pi$ interaction, etc., contribute to the aggregation of nanoparticles. This is a challenge to obtain stable dispersion. Therefore during the synthesis of CuS, different types of stabilizers have been used to get stable dispersion. On standing, the particles in the dispersion were precipitated out when the reactions were performed below critical micelle concentration (CMC) value of CTAB. CuS nanostructures were prepared by changing the stabilizer concentration from 0.05 to 0.1 mM.

A. XRD analysis

The crystallographic structures of CTAB stabilized CuS nanostructures are investigated by XRD analysis. Figure 1 (a-c) shows the XRD patterns of CuS nanostructures by using various concentrations of (CTAB) cationic surfactant.

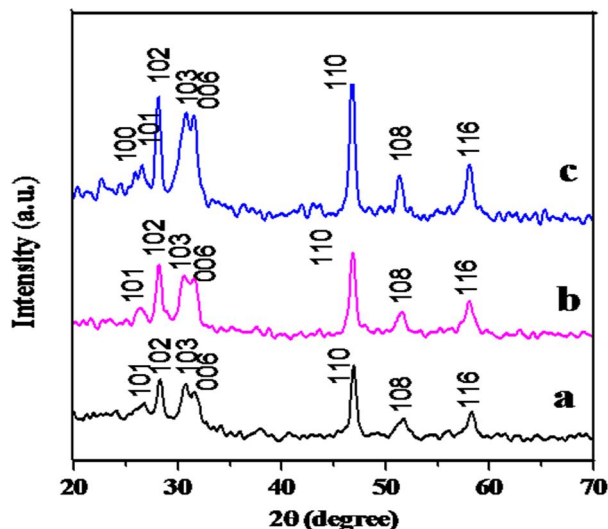


Fig.1 The XRD patterns of CuS assisted with CTAB
(a) 0.05, (b) 0.07 and (c) 0.1 mM

All the diffraction peaks can be indexed as 2θ values positioned at 26.13° , 27.11° , 29.54° , 31.95° , 32.65° , 47.78° , 52.14° and 59.25° corresponding to the (hkl) planes of (100), (101), (102), (103), (006), (110), (108) and (116) of covellite CuS in good crystalline quality, which is consistent with the hexagonal CuS standard spectrum, with lattice constants of $a=3.792 \text{ \AA}$ and $c=16.344 \text{ \AA}$ are well matches with the standard card (JCPDS No.06-0464) [23]. No observable impurity phases were seen in the XRD spectra, it indicating the formation of hexagonal phase of CuS only. According to the estimation of the scherrer equation, the average particle size of various concentrations of (0.05, 0.07 and 0.1mM) CTAB assisted CuS nanostructures are 24, 19 and 14 nm respectively.

B. XPS Analysis

To further investigate the (0.1mM) CTAB-CuS products were analyzed by X-ray photo-electron spectroscopy (XPS) for the evaluation of their composition and purity. No peaks of any impurities are detected in the XPS spectra, indicating the high purity of the product. Fig. 2a and b shows the high-resolution XPS spectra of Cu 2p and S 2p respectively. Fig.2a shows the Cu 2p_{3/2} peak is found at 931.59 eV and Cu 2p_{1/2} peak is found at 951.37 eV which corresponds to CuS.

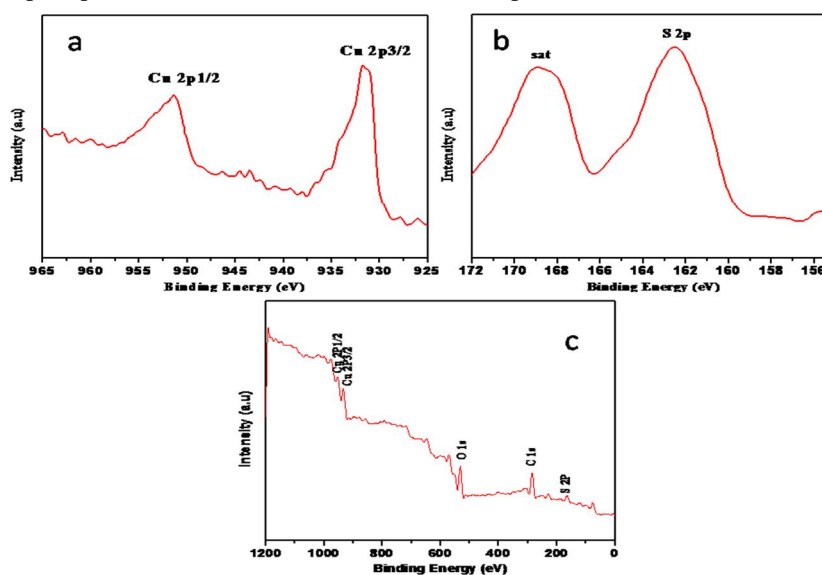


Fig. 2 XPS spectra of (0.1mM) CTAB stabilized CuS nanostructures
(a) Cu 2p and (b) S 2p (c) full spectrum

Fig. 2b presents the XPS spectrum for the S 2p state, the peak located at a binding energy of 162.53 eV corresponds to Cu - S atom [24]. The satellite structure is not detected, except that there is some asymmetry in the peak shape toward higher binding energies. As shown in fig.2c the survey spectrum of the sample, this reveals that all the peaks have been marked. Evidently, the existence of all the peaks can be ascribed to the elements Cu 2p, S 2p and C 1s as well as O 1s elements from reference and oxygen in the sample is likely due to their exposure to the atmosphere. Hence from XPS analysis, it can confirm the presence of all desired elements used for the preparation of CuS nanostructures. In the near-surface range, the chemical composition of the product is Cu and S which is well agreement with this experiment. From the XPS spectrum, there is no other elements are found it indicating the high purity of the sample.

C. Sem/Eds

The surface morphology study reveals that the formation of CTAB/CuS microstructures to a size of 1 μ m as shown in figure 3. The SEM images confirms that the average diameters of the porous nanostructure of (0.05) CTAB-CuS, (0.07) CTAB-CuS and (0.1mM) CTAB-CuS samples are about 24-27 nm, 19-22 nm and 14-19 nm respectively.

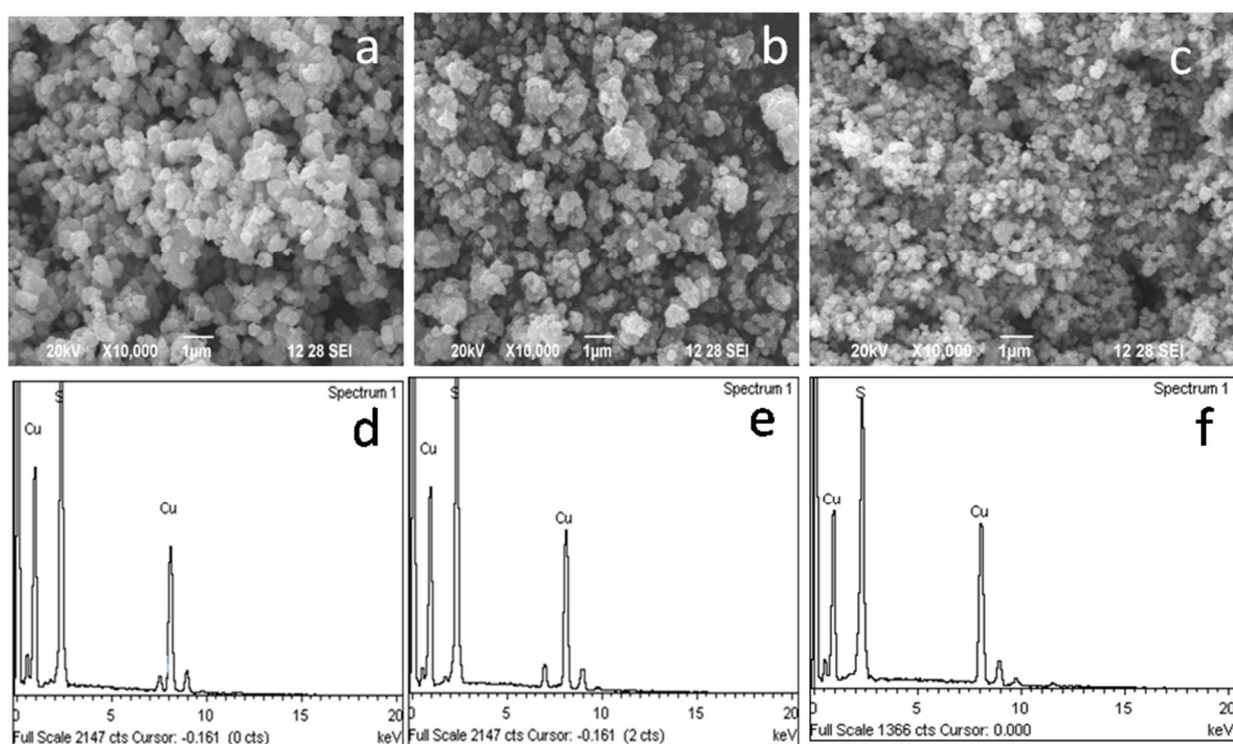


Fig.3 SEM image of CuS assisted with CTAB (a) 0.05, (b) 0.07 and (c) 0.1 mM and (d-f) are corresponding EDS spectra

The SEM images of the products obtained at 130°C in fig. (3(a-c)) are found to be sphere with flake-like nanostructures. The SEM image shown in figure 3(c) clearly shows that evenly dispersed with minimal cluster formation of flower-like morphology (0.1mM) CTAB-CuS microstructures. The EDS spectra shown in Fig.3(c, f and i) confirmed that the presence of Cu and S peaks only. The molar ratio of Cu and S was 1:2, well agreeing with the stoichiometry of CuS.

D. TEM

Fig.4 (a-c) shows the TEM images of porous (0.1mM) CTAB stabilized CuS nanostructures. The morphology of (0.1mM) CTAB-CuS consists of thinly stacked flakes of shapes with well defined structures at the edges and the average diameter of around 30nm. TEM images clearly show flower-like morphology. The corresponding selected area electron diffraction (SAED) pattern (fig. 4(d)) reveals that the crystalline structure can be indexed to the (101), (102), (103), (110), (108) and (116) planes of the hexagonal CTAB-CuS nanostructures. These results are confirms the XRD observation.

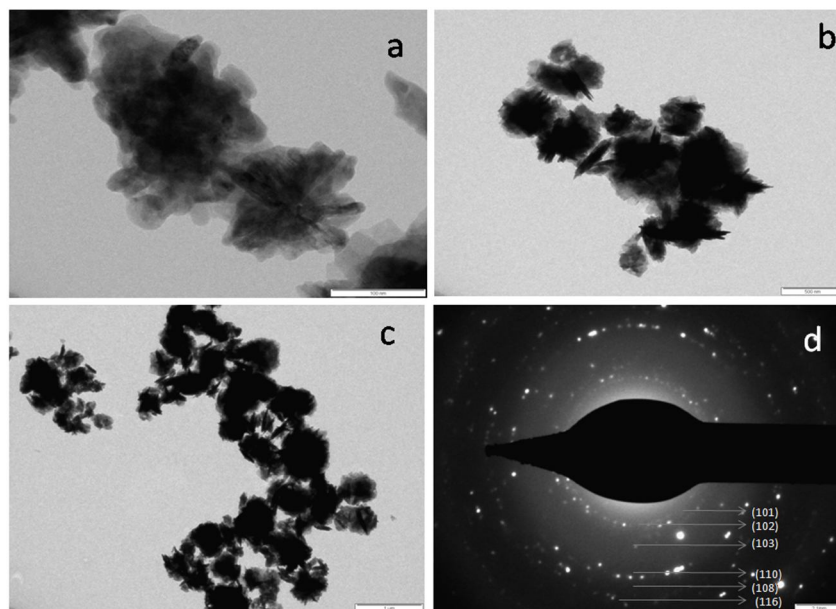


Fig.4 (a)-(c) TEM image of CTAB (0.1mM)-CuS nanostructures (d) SAED pattern

E. Electrochemical studies

The capacitive behavior of the various concentrations of CTAB stabilized CuS electrodes were evaluated by cyclic voltammetry (CV) tests in a three-electrode configuration system with a 2M KOH aqueous electrolyte. Fig.5.(a-c) shows the cyclic voltammograms (CV) of a (0.05)CTAB-CuS, (0.07) CTAB-CuS and (0.1mM) CTAB-CuS electrode with a potential range between 0.0 to 0.5 V (vs SCE) at different scan rates such as 5, 10, 20 and 50 mV/s.

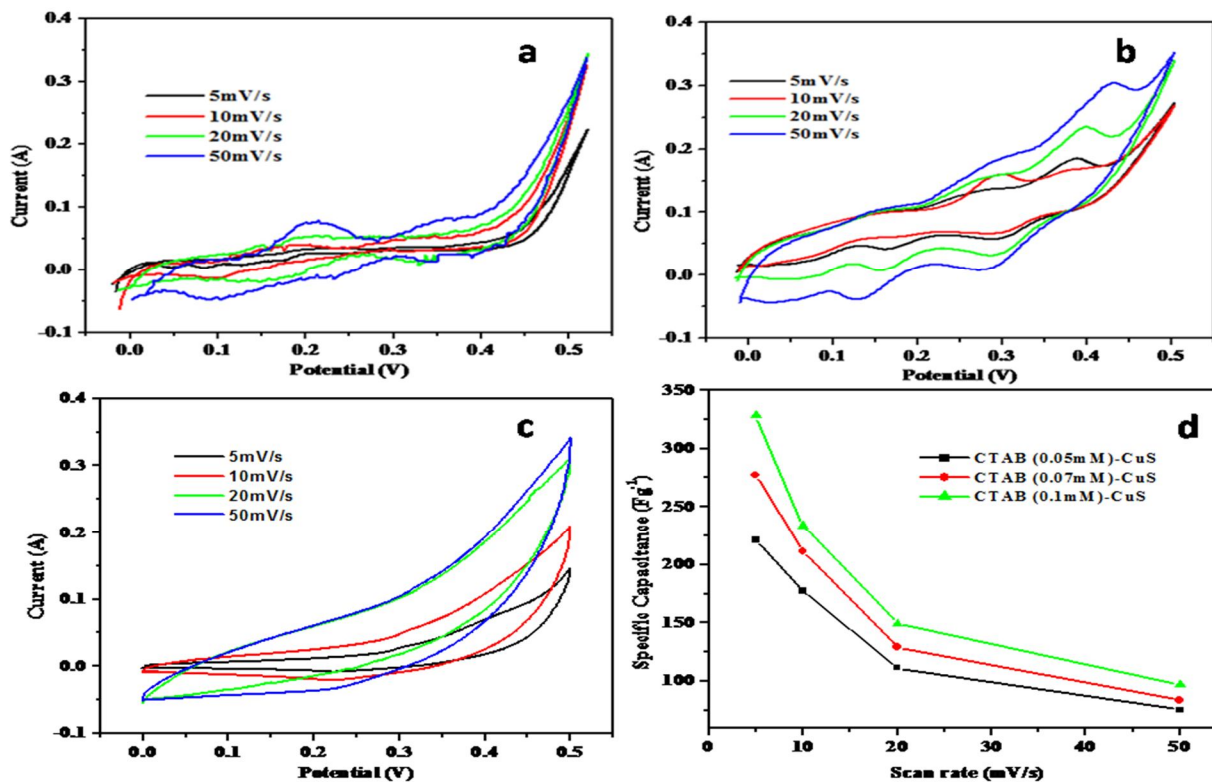


Fig.5 CV

curves of (a) (0.05) CTAB-CuS , (b) (0.07) CTAB-CuS and (c) (0.1 mM) CTAB-CuS (d) specific capacitance calculated from the CV curves

Fig.5 (a, b) shows the CV curves of modified (0.05 and 0.07mM) CTAB-CuS electrodes. The tendency towards a box-like shape and some redox curves are observed of these curves indicates nearly ideally capacitive behavior of the CuS nanostructures. The test was carried out under a fixed potential window, 0.1–0.5 V. Fig.5c demonstrates the CV curves of modified (0.1mM) CTAB-CuS electrode roughly rectangular shape superimposed with broad faradaic curve in the range of 0.1 to 0.4 V [25]. Besides, as the scan rates varies between 5 and 50 mV/s, the shapes of the CV curves do not significantly change and still shows rectangular features. This shows the good high-rate capability of the (0.1mM) CTAB-CuS nanostructures. This indicates the coexistence of electrical double layer and faradic pseudo capacitances for modified CuS electrode [26, 27]. Compared with other electrodes, the area under the CV curve is greatly higher for the (0.1mM) CTAB-CuS electrode has the largest CV area, indicating the highest levels of stored charge. The specific capacitance of the three CTAB (0.05, 0.07 and 0.1mM)-CuS electrodes can be calculated by the following formula

$$C_s = \frac{Q}{\Delta V \cdot m}$$

Where C_s represents the specific capacitance, Q is the anodic and cathodic charges on each scanning, m is the mass of the active material (g) in the electrodes and ΔV is the applied voltage window of the voltammetric curve (mVs^{-1}). The specific capacitance values were found to increase in the order of (0.05)CTAB-CuS (221.23Fg^{-1}) < (0.07)CTAB-CuS(277.11Fg^{-1}) < (0.1mM)CTAB-CuS(328.26Fg^{-1}) at a scan rate of 5mV/s in 2M KOH aqueous electrolyte solution. This result can be attributed to the largest specific surface area of the (0.1mM) CTAB-CuS sample.

IV. CONCLUSION

In summary, three different concentrations of CTAB used as soft templates to control the self-assembly process of CuS nanostructures were successfully prepared. The reactions were carried out in the reaction temperature 130°C via a hydrothermal method. It was found out that stabilizer on the CuS affect the morphologies, size and yields of the products, that is flower-like CuS nanostructures were obtained after 10hrs. Among the three CuS electrodes has the highest specific surface area and optimal electrochemical properties because of the mono dispersive mesoporous distribution. Thus the as-obtained porous (0.1mM) CTAB-CuS electrode reveals a high specific capacitance of 328.26Fg^{-1} at scan rate of 5mVs^{-1} is highly promising electrode material for energy storage applications (Supercapacitor).

V. ACKNOWLEDGEMENT

The authors appreciatively thanks to the financial support afford by University grants commission (UGC), India, (F.No- 43-533/2014 (SR)).

REFERENCES

- [1] Yang Z., Ren J., Zhang Z., Chen X., Guan G., Qiu L., Zhang Y., Peng H., Recent advancement of nanostructured carbon for energy applications, Chem. Rev. **2015**, 115, 5159-5223.
- [2] Yan J., Wang Q., Wei T., Fan Z., Recent advances in design and fabrication of electrochemical supercapacitors with high energy densities, Adv. Energy Mater. **2014**, 4, 1300816.
- [3] Su D., Pan L., Fu X., Ma H., Facile synthesis of CNC-MnO₂ hybrid as a supercapacitor electrode, Appl. Surf. Sci. **2015**, 324, 349-354.
- [4] Zhao S., Liu T., Hou D., Zeng W., Miao B., Hussain S., Peng X., Javed M.S., Controlled synthesis of hierarchical birnessite-type MnO₂ nanoflowers for supercapacitor applications, Appl. Surf. Sci. **2015**, 356, 259-265.
- [5] Hsu Y.K., Chen Y.C., Lin Y.G., Synthesis of copper sulfide nanowire arrays for high-performance supercapacitors, Electrochim. Acta **2014**, 139, 401-407.
- [6] Peng H., Ma G., Sun K., Mu J., Wang H., Lei Z., High-performance supercapacitor based on multi- structural CuS@polypyrrole composites prepared by in situ oxidative polymerization, J. Mater. Chem. A **2014**, 2, 3303-3307.
- [7] Peng H., Ma G., Mu J., Sun K., Lei Z., Controllable synthesis of CuS with hierarchical structures via a surfactant-free method for high-performance supercapacitors, Mater. Lett. **2014**, 122, 25-28.
- [8] Wang H., Liang Y., Li Y., Dai H., Co_{1-x}S-Graphene Hybrid: A High-Performance Metal Chalcogenide Electrocatalyst for Oxygen Reduction, Angew., Chem. Int., Ed. **2011**, 50, 10969.
- [9] Seyede S. K., Hossein D., Ca-doped CuS/graphene sheet nanocomposite as a highly catalytic counter electrode for improving quantum dot-sensitized solar cell performance, RSC Adv. **2016**, 6, 10880.
- [10] Jiang H., Ma J., Li C.Z., Mesoporous Carbon Incorporated Metal Oxide Nanomaterials as Supercapacitor Electrodes, Adv. Mater. **2012**, 24, 4197-4202.
- [11] Hao L., Li X., Zhi L., Carbonaceous Electrode Materials for Supercapacitors, Adv.Mater. **2013**, 25, 3899-3904.
- [12] Wu D., Xu S., Lia M., Zhang C., Zhu Y., Xu Y., Zhang W., Huang R., Qi R., Wang L., Chu P. K., Hybrid MnO₂/C nano-composites on a macroporous electrically conductive network for supercapacitor electrodes, J. Mater. Chem A. **2015**, 3, 16695-16707.
- [13] Jayalakshmi M., Rao M.M., Synthesis of zinc sulphide nanoparticles by thiourea hydrolysis and their characterization for electrochemical capacitor applications, J. Power Sources. **2006**, 157, 624-629.

- [14] Tsamouras D., Kobotiatis L., Dalas E., Sakkopoulos S., An impedance study of the metal sulfide $\text{Cu}_x\text{Zn}_{(1-x)}\text{S}$ electrolyte interface, *J. Electroanal. Chem.* **1999**, 469, 43–47.
- [15] Wang B., Park J., Su D., Wang C., Ahn H., Wang G., Solvothermal synthesis of CoS_2 –graphene nanocomposite material for high-performance supercapacitors, *J. Mater. Chem.* **2012**, 22, 15750–15756.
- [16] Ratanatawanate C., Bui A., Vu K., Balkus K.J., Low-Temperature Synthesis of Copper(II) Sulfide Quantum Dot Decorated TiO_2 Nanotubes and Their Photocatalytic Properties, *J. Phys. Chem. C* **2011**, 115, 6175–6180.
- [17] Jiang X., Xie Y., Lu J., He W., Zhu L., Qian Y., Preparation and phase transformation of nanocrystalline copper sulfides (Cu_9S_8 , Cu_7S_4 and CuS) at low temperature, *J. Mater. Chem.* **2000**, 10, 2193–2196.
- [18] Chen L., Yu W., Li Y., Synthesis and characterization of tubular CuS with flower-like wall from a low temperature hydrothermal route, *Powder Technol.* **2009**, 191, 52–54.
- [19] Setkus A., Galdikas A., Mironas A., Imkiene I. S, Ancutiene I., Janickis V., Kaciulis S., Mattogno G., Ingo G. M., Properties of Cu_xS thin film based structures: influence on the sensitivity to ammonia at room temperatures, *Thin Solid Films.* **2001**, 391, 275–281.
- [20] Shen X.P., Zhao H., Shu H.Q., Zhou H., Yuan A.H., Self-assembly of CuS nanoflakes into flower-like microspheres: Synthesis and characterization, *J. Phys. Chem. Solids.* **2009**, 70, 422–427.
- [21] Huang Y., Xiao H., Chen S., Wang C., Preparation and characterization of CuS hollow spheres, *Ceramics International.* **2009**, 35, 905-907.
- [22] Surekha P., Geetha D., Ramesh P.S., One-pot synthesis of CTAB stabilized mesoporous cobalt doped CuS nano flower with enhanced pseudocapacitive behavior, *J Mater Sci: Mater Electron.* **2017**, 28, 15387-15397.
- [23] Z. Liying, X. Yi, Z. Xiuwen, L. Xiang, Z. Gui'en, Fabrication of novel urchin-like architecture and snowflake-like pattern CuS , *J.Crystal growth*, 260 (2004): 494-499.
- [24] M. Tanveer, Chuanbao Cao, Zulfiqar Ali, Imran Aslam, Faryal Idrees, Waheed S. Khan, Faheem K. But, Muhammad Tahira, Nasir Mahmood, Template Free Synthesis of CuS Nanosheet-based Hierarchical Microspheres: An Efficient Natural Light Driven Photocatalyst, *Cryst Eng Comm.* 16 (2014): 5290-5300.
- [25] M. Silambarasan, P. S. Ramesh, D. Geetha, V. Venkatachalam, A report on 1D MgCo_2O_4 with enhanced structural, morphological and electrochemical properties, *J Mater Sci: Mater Electron*, 28 (2016): 6880-6888.
- [26] A. Wang, H. Wang, S. Zhang, C. Mao, J. Song, H. Niu, B. Jin, Y. Tian, Controlled synthesis of nickel sulfide/ graphene oxide nanocomposite for high performance supercapacitor, *Appl. Surf. Sci* 282 (2013) 704-708.
- [27] S.S. Shindea, G.S. Gunda, D.P. Dubalb, S.B. Jamburea, S.B. Lokhande, Morphological modulation of polypyrrole thin films through oxidizing agents and their concurrent effect on supercapacitor performance, *Electrochim. Acta*, 119 (2014): 1–10.



10.22214/IJRASET



45.98



IMPACT FACTOR:
7.129



IMPACT FACTOR:
7.429



INTERNATIONAL JOURNAL FOR RESEARCH

IN APPLIED SCIENCE & ENGINEERING TECHNOLOGY

Call : 08813907089  (24*7 Support on Whatsapp)